PAPER

NJC
www.rsc.org/njc

Active Ru catalysts in carbene chemistry: A kinetic study of carbene formation and an evaluation of selective cyclopropanation

Jeroen Van Craenenbroeck, Koen Van Isterdael, Carl Vercaemst and Francis Verpoort*

Department of Physical and Inorganic Chemistry, Ghent University, Krijgslaan 281 (S3), 9000 Ghent, Belgium. E-mail: francis.verpoort@UGent.be; Fax: (+032) 09 2644983; Tel: (+032) 09 2644436

Received (in Montpellier, France) 18th October 2004, Accepted 14th April 2005
First published as an Advance Article on the web 9th June 2005

p-Cymene–Ru catalysts containing bidentate *N*,*O*-Schiff base ligands, known as active catalysts in various reactions, are studied in relation to the cyclopropanation of olefins with ethyl diazoacetate. The study is divided into two parts. (1) The decomposition of ethyl diazoacetate is followed by FT-IR and elementary kinetic parameters calculated. (2) The selectivity and diastereoselectivity of cyclopropanation is then determined by GC analysis. The catalysts and ligands are fully characterized by FT-Raman and NMR spectroscopy. Furthermore, catalyst stabilities are checked by means of TGA measurements. It is found especially that the electronic properties of the ligands determine catalyst performance.

1. Introduction

One of the most elegant methods for synthesising cyclopropane products available today is the transition metal catalyzed decomposition of diazo compounds. This method is thought to involve the transfer of an *in situ*-generated carbene to an olefin.[1] Rh and Cu catalysts with a wide range of ligands have been extensively studied for this reaction.[2] Recently the focus has moved to Ru catalysts as cheaper alternatives to Rh, and promising results are already being reported.[3] Over recent years, the reported coordination chemistry of the transition metals has become very complex; many catalysts designed to facilitate asymmetric cyclopropanation now consisting of steric and/or rigid, tri or tetradentate ligands containing chiral entities.[4,5] Unfortunately due to a high specificity, their application to other classes of reaction are rarely reported,[6] and in most cases they are restricted only to cyclopropanation reactions.

In this study we report the activity of Ru catalysts with proven activity towards olefin metathesis, radical polymerization (ATRP), enol-ester synthesis, vinylation and dimerisation reactions of different kinds of olefins.[7] As the proposed reaction pathway for cyclopropanation shows a high similarity to metal catalyzed olefin metathesis, where a reaction between a metal carbene and an olefin occurs as well as dimerisation,[8] we explore the activity of these existing catalysts towards cyclopropanation rather than developing new ones.

The coordinating atoms of *N*,*O*-Schiff bases, an imine nitrogen atom and a phenolate oxygen atom, exhibit quite different behaviours. The former is thought to be a soft donor atom (in terms of hard–soft acid–base coordination principle, HSAB), stabilizing the lower oxidation states of Ru. The latter stabilizes higher oxidation states because of its harder, HSAB-donating properties.[9] These two features make *N*,*O*-Schiff base ligands valuable candidates for occupying the ligand periphery of catalysts, since they have the ability to stabilize reactive intermediary species in a variety of oxidation states.

The precursor materials and the catalysts are easy to prepare, and show a high tolerance to air and moisture. By controlling the reaction parameters we are able to channel the catalytic activity by suppressing metathesis and dimerisation, the major carbene side reactions, and favour instead cyclopropanation.

2. Results

A detailed characterization of the ligands and catalysts has already been described.[7c,10] An overview of the catalyst's structures are given in Scheme 1.

Thermogravimetric analysis

Thermogravimetric analysis (TGA) of the catalysts gives an idea about the ligand coordination strength. All catalyst samples showed a large mass loss in the temperature range 170–250 °C; for example, the result of one TGA experiment is shown in Fig. 1 (TGA plot and its derivative for catalyst **C3**). The decoordination temperature, T_{dc}, is defined as the maxima of the derivative curve, and its value for each catalyst is shown in Table 1.

FT-IR kinetic measurements

It is generally accepted that the cyclopropanation of olefins by diazo compounds proceeds in two steps (Scheme 2). Firstly, a diazo compound decomposes, releasing N_2, and forming a reactive metal carbene. This is followed by transfer of the carbene to the olefin.

Here we report the results of the catalytic decomposition of ethyl diazoacetate (EDA), monitored *in situ* by FT-IR. The reaction is irreversible due to the release of N_2 and therefore should proceed as long as EDA is present. Thermal decomposition of EDA was observed above 80 °C, in agreement with the work of other researchers.[11] A correction for this reaction was necessary at higher temperatures.

We performed a kinetic analysis, not to seek new mechanistic findings, but to obtain a clearer view of the relationship between the properties of the ligands and the reactivity of their respective catalytic systems towards the decomposition of EDA. Moreover, because the reaction mechanism is largely understood, researchers today are more focused on the yield and selectivity of cyclopropanation. This means it is rare that

DOI: 10.1039/b416020g

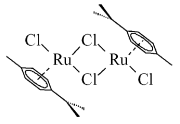

C0: $[RuCl_2(p\text{-cymene})]_2$

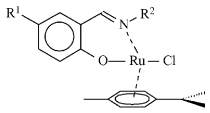

C1: R^1 = H; R^2 = Me
C2: R^1 = H; R^2 = *t*Bu
C3: R^1 = H; R^2 = 2,4,6-trimethylphenyl
C4: R^1 = H; R^2 = 4-bromo-2,6-dimethylphenyl
NC1: R^1 = NO_2; R^2 = Me
NC2: R^1 = NO_2; R^2 = *t*Bu
NC3: R^1 = NO_2; R^2 = 2,4,6-trimethylphenyl
NC4: R^1 = NO_2; R^2 = 4-bromo-2,6-dimethylphenyl

Scheme 1 An overview of the catalyst's structures.

kinetic data such as rate constants and activation energies are published,[12] despite their fundamental importance.

All concentration *vs.* time plots were exponentially fitted using the program Igor Pro. The high correlation (>99%) of experimental results that fitted the curve confirmed the kinetic behaviour. From the fitted exponential curve, we were able to derive several kinetic parameters. All kinetic calculations were based on the initial part of the reaction, *i.e.* the very short time after the reaction has started, the measurements for this stage showing a log [EDA] decrease over time, indicating a first order reaction in EDA.

The observed reaction rate, r_{obs}, was proportional to the diazo concentration, and by determining this rate, r_{obs}, and the observed rate constant k_{obs}, we calculated the reaction rate constant k_{calc} ($[Ru]_0$ is the original catalyst concentration *i.e.* at time zero):

$$k_{calc} = \frac{k_{obs}}{[Ru]_0} \quad (1)$$

As a first step, we checked the decomposition activity at 60 °C for the different catalysts. The EDA conversions are given in Fig. 2A and B.

Based on the mathematical expression ($y = a \times \exp(-bx)$) of the fitted curve, we determined the slopes *i.e.* the reaction rate, r_{obs}, at 0, 0.01, 0.02, 0.03 and 0.04 min after the start of the reaction. The rate constant, k_{calc}, was thus calculated and the results summarized in Table 2. The order in EDA was 1 in all cases (±0.016 experimental error) and this value was taken as a measure of the accuracy of the fitting process.

To obtain a more detailed view of the catalysts' activity, we followed the decomposition of EDA at different temperatures. From these experiments, an activation energy based on the Arrhenius equation could be derived. The influence of temperature was investigated for two catalysts, **C1** and **NC1**, and the results are shown in Fig. 3A and B, and Table 3.

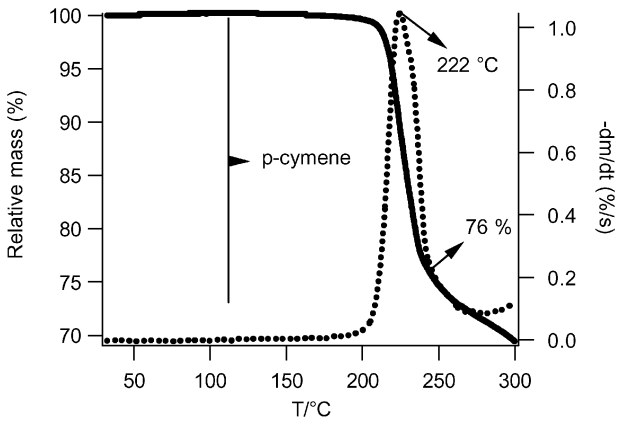

Fig. 1 TGA plot and its derivative for sample **C3**. The temperature program ran from room temperature to 300 °C at 10 °C min^{-1} under a He atmosphere.

Table 1 Decoordination temperatures (T_{dc})

Sample	T_{dc}/°C[a]	Sample	T_{dc}/°C[a]
C0	266.1		
C1	212.4	**NC1**	230.2
C2	179.0	**NC2**	193.5
C3	222.7	**NC3**	229.9
C4	237.0	**NC4**	248.1

[a] Temperature of the maxima of the TGA derivative plot, *i.e.* the temperature at which decoordination of *p*-cymene occurs under a He atmosphere. Experimental error = ±0.1 °C, the temperature difference between a pair of adjacent data points.

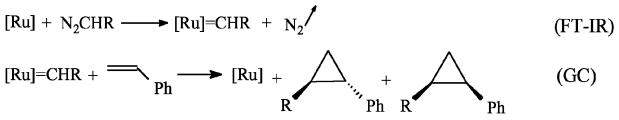

Scheme 2 General cyclopropanation sequence.

GC-measurements

Olefin metathesis and dimerisation reactions are the most common side reactions of cyclopropanation (Table 4). Due to the known activity of our systems towards these reactions, we investigated whether it was possible to favour cyclopropanation over them by adjusting the reaction parameters. Dimerisation could be suppressed by manipulation of the EDA addition rate to the reaction, and by the use of an excess of olefin. We analysed a sample using IR measurements, thus checking the influence of the EDA addition rate (Table 4, entry $\mathbf{C1}_{IR}$).

Metathesis reactions could be suppressed by performing the reaction in an inert solvent such as toluene instead of pure olefin.

In our first experiment, the activity and diastereoselectivity of the different catalysts towards cyclopropanation were checked at 60 °C (Table 4). The enantioselectivity was not determined since high levels were not expected.

Since the nature of the olefin is thought to be more influential in carbene transfer than it is for the decomposition of EDA, it was considered worthwhile investigating the cyclopropanation activity of other olefins We therefore performed a second experiment with catalyst **C1**, the results of which are shown in Table 5.

3. Discussion

According to TGA, the least stable fraction seems to be the η^6-coordinated arene group *p*-cymene (error ±5%). From this agreement between the catalysts, we can get some useful information about the complex's nature, since the coordination strength of the arene group reflects the electronic properties of the ligand's periphery.

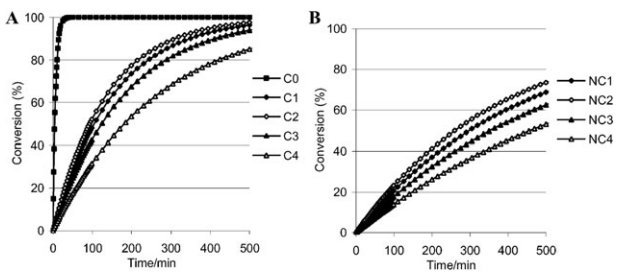

Fig. 2 A: Decomposition of EDA at 60 °C for catalysts **C0–C4**. Conditions: 1 μmol catalyst, catalyst : EDA : substrate = 1 : 125 : 2500. B: Decomposition of EDA at 60 °C with **NC1–NC4**. Conditions: 1 μmol catalyst, catalyst : EDA : substrate = 1 : 125 : 2500.

Table 2 Rate constant, k_{calc}, for each catalyst

Catalyst	k_{calc}/l mol^{-1} s^{-1} [a]	Catalyst	k_{calc}/l mol^{-1} s^{-1} [a]
C0	3353.7[b]		
C1	87.4	**NC1**	30.8
C2	95.3	**NC2**	35.3
C3	72.3	**NC3**	25.9
C4	50.6	**NC4**	20.0

[a] $k_{calc} = k_1K_{eq} = k_2k_1k_1^{-1}$. [b] $k_{calc,C0} = l^{1/2}$ mol$^{-1/2}$ s^{-1}.

When applying different Schiff base ligands with strong N,O donors, T_{dc} could be taken as a measure of the coordination strength of the arene group. In this way it was found that the presence of a strong electron-withdrawing NO_2 group on the salicyl ring reduced the donor capacity of the phenolate O atom. This resulted in higher T_{dc} values for the nitro Schiff bases. The properties of the N-donor, on the other hand, are determined by the substituents on the imine nitrogen atom. Due to the relatively soft HSAB properties of this donor, the correlation with electronic properties was a more difficult one to make. The difference between Me (**C1**) and ^{t}Bu (**C2**) could be explained by their relative electron-donating properties, ^{t}Bu > Me; although, according to this reasoning, one should expect lower values of T_{dc} for the aromatic N-substituents (**C3** and **C4**) than the aliphatic ones (**C1** and **C2**). However, in case of an aromatic substituent, the Schiff base ligand becomes a completely conjugated system, resonance effects are induced, and the donating properties of the nitrogen atom diminish as a result. The resonance effect is obvious when a *p*-bromo substituent is added to the aniline ring (**C3** *vs.* **C4**).

The trend observed in the stability fits well with elementary theoretical expectations based on electronic properties of the Schiff base ligand. The stronger the electron donating properties of the ligand, the higher the electron density on the Ru centre, the weaker the arene coordination, and the lower the value of T_{dc}.

However, deductions from the TGA data (Table 1), relating to the relative activity of different catalysts, should be made carefully since the experiments were conducted in an inert atmosphere, not in solution. Therefore only the bonding properties in relation to electronic stabilization of the Ru centre by the coordinating ligands could be made. No reasonable conclusions concerning the steric properties of the catalysts could be drawn.

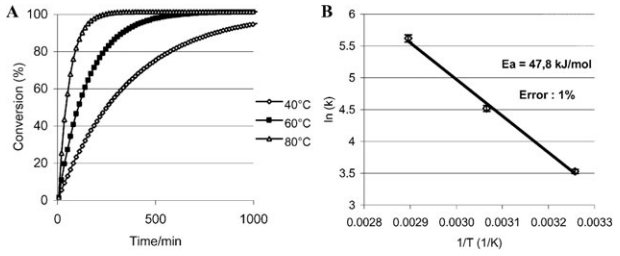

Fig. 3 A: The influence of temperature on the decomposition activity of catalyst **C1**. Conditions: 1 μmol catalyst, catalyst : EDA : substrate = 1 : 125 : 2500. B: The Arrhenius plot for **C1**.

Table 3 k_{calc}[a] (l mol^{-1} s^{-1}) at a variety of temperatures for catalysts **C1** and **NC1**

T/°C	$k_{calc,C1}$[a]	$k_{calc,NC1}$[a]
40	32.6	—
60	87.4	27.7
80	263.3	54.4
100	—	129.1

[a] $k_{calc} = k_1K$.

Table 4 Selectivity towards cyclopropanation

Catalyst	%C[a]	%D[b]	%M[c]	*trans* : *cis*
C0	59	27	14	1.4 : 1
C1	73	19	8	2.3 : 1
C2	75	18	7	2.8 : 1
C3	76	20	4	2.4 : 1
NC1	65	25	10	1.9 : 1
NC2	69	31	10	1.8 : 1
NC3	72	20	8	1.5 : 1
NC4	73	20	7	1.7 : 1
C1$_{IR}$[d]	52	42	6	2.3 : 1

[a] % Cyclopropanation. [b] % Dimerisation. [c] % Metathesis. [d] EDA is added all at once.

Therefore we had to look to the IR results for the EDA decomposition (Fig. 4A and B). The trend in decomposition activity (by FT-IR) appears to correlate with the trend in lability of the arene ligand (by TGA), implying that for these systems, the steric influence over the decomposition activity is negligible. The dominance of the electronic properties is clear when comparing the relative small differences in activity when larger *N*-substituents are used (C_1 *vs.* C_2 and C_3) with the large decrease in decomposition activity when a *p*-NO_2 substituent on the salicyl ring is applied (catalyst type C *vs.* NC).

The absence of a dominant steric factor provides support for a dissociative mechanism. From the correlated results of the stability experiments (TGA) and EDA decomposition activity (FT-IR), we therefore assume that the EDA decomposes *via* a dissociative mechanism by preliminary de- or recoordination of the arene group to activate the catalyst and to minimize the steric hindrance between the carbene and substrate. The activation process, and so the nature of the activated species Ru*, remains unclear, but most probably involves a decoordination or recoordination from η^6 to η^4 or lower.

To gain a clearer view of the general decomposition activity, we performed experiments at a range of temperatures (Fig. 3A and B). Comparing the reasoning made above with that obtained from the temperature dependence studies of **C1** and **NC1** (we assumed for this comparison that no differentiating steric factor was present, since both systems have the same substituent at nitrogen), we apparently obtained contradictory results; **NC1** showed a lower decomposition activity than **C1**, in accordance with the observed stability from our TGA experiments, but a smaller E_a was found (*i.e.* a smaller temperature dependence).

The reaction occurred in solution and therefore has a notable implication; the higher the electron donating properties of the Schiff base, the larger the stabilizing effect after arene decoordination, and thus the less reactive the resulting species. This implication predicts that NO_2-substituted Schiff base systems (**NC1–NC4**) produced more reactive Ru* intermediates. An indication of this can be found in the GC results (Table 4) where nitro systems showed lower selectivities towards cyclopropanation and lower diastereoselectivities, implying more reactive intermediary species. Based on these

Table 5 The selectivity of cyclopropanation with different substrates and catalyst **C1**

Substrate	%C[a]	%D[b]	%M[c]	*trans* : *cis*
Styrene	73	19	8	2.3 : 1
4-Methoxystyrene	74	18	8	2.4 : 1
4-Chlorostyrene	68	21	11	2.3 : 1
cis-Cyclooctene	30	69	<1	10 : 1
1-Octene	42	57	<1	3.1 : 1

[a] % Cyclopropanation. [b] % Dimerisation. [c] % Metathesis.

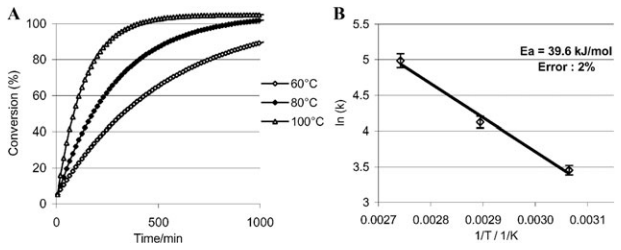

Fig. 4 A: The influence of temperature on the decomposition activity of catalyst **NC1**. Conditions: 1 μmole catalyst, catalyst : EDA : substrate = 1 : 125 : 2500. B: Arrhenius plot of **NC1**

statements, we propose a plausible mechanism, containing the preceding equilibrium, to explain the results in a more fundamental way (Scheme 3).

The first step is an dissociative–associative equilibrium, shifted in favour of the associated complex. Once the catalyst is activated, a reactive species, Ru*, is formed. Reaction of the carbene, RuC, after decomposition of an EDA molecule, E, with a substrate molecule, S, results in cyclopropanation product, P_c. When another EDA molecule is involved in the carbene reaction, dimerisation product, P_d, is formed. Metathesis products are obtained only in very low proportions and therefore have not been included in this mechanism.

When obtaining a rate equation showing first order kinetics in EDA, two assumptions can be justified. Firstly, the dissociative–associative equilibrium is very rapid. Secondly, a steady state in the intermediary carbene species, RuC, is assumed. If the association–dissociation step is rate determining, the rate would not depend on EDA concentration. The second assumption is justified due to the fact that the intermediary carbene species, RuC, for these systems is not detected *in situ* by NMR. This means that the concentration of carbene species present is very small.

There are three implications leading from these assumptions: (1) The carbene formation step must be rate determining (and thus the observed rate equals the rate of product formation because of the reactive nature of RuC). (2) Due to the nature of the equilibrium, the actual concentration of associated complex, RuX, can be taken as its initial concentration. (3) The concentration of Ru* is small and constant over time, *i.e.* steady state.

Using the reaction sequence below (Scheme 4), we have deduced a rate equation which is consistent with our experimental data:

$$\text{Observed rate} = r_2 = K_{eq}k_2[\text{Ru}]_0[\text{E}] = k_{obs}[\text{E}] \qquad (2)$$

The observed rate constant, k_{obs}, consists of two terms: the constant of the preceding equilibrium, K_{eq}, and the rate constant of the actual EDA decomposition, k_2. From r_2 (eqn. (2)), the calculated rate constant k_{calc} (eqn. (1)) and the reaction sequence (Scheme 4), it is obvious that the reaction rate depends on the decomposition rate of EDA and on a thermodynamic equilibrium.

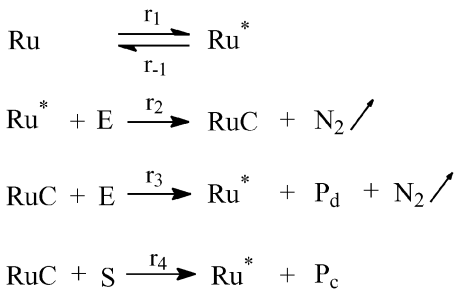

Scheme 3 Proposed reaction mechanism based on experimental data.

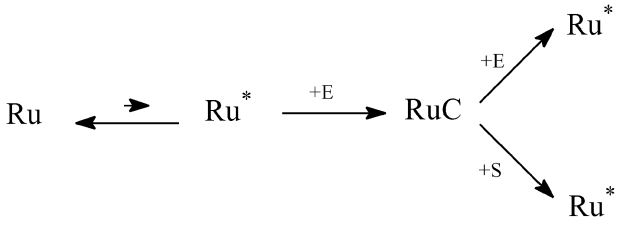

Scheme 4 Reaction sequence.

The temperature dependence of the calculated rate constant k_{calc} can now be expressed as:

$$E_{a,calc} = \Delta H_{eq} + E_{a,2} \qquad (3)$$

So for a given catalytic system, the enthalpic term, ΔH_{eq}, of the calculated activation energy approaches the electronic properties of the Schiff base ligand from a thermodynamic point of view, since these properties influence the complex's stability and thus Ru* concentration. The second term, $E_{a,2}$, also reflects the electronic properties, although in a kinetic manner, since they are responsible for the reactivity of the activated Ru centre, Ru*, towards EDA.

A measure of ΔH_{eq} can be taken from the bonding enthalpies, ΔH_b; the value being larger when the arene coordination is stronger. On the other hand, we have expressed the coordination strength (*i.e.* bonding enthalpies) as decoordination temperatures, T_{dc}, obtained by TGA.

We have found from Table 1, Fig. 4A and B that:

$$T_{dc,NC}(\propto \Delta H_{eq,NC}) > T_{dc,C}(\propto \Delta H_{eq,C}) \qquad (4)$$

$$E_{a,NC,calc} < E_{a,C,calc} \qquad (5)$$

According to eqn. (3), this means that:

$$E_{a,2,NC} \ll E_{a,2,C} \qquad (6)$$

The temperature has a smaller effect on the actual decomposition of EDA by Ru* when nitro systems are used. This is a more fundamental indication of the earlier assumptions: nitro systems provide more reactive intermediary Ru* species.

From this deduction, it is clear that the observed activity depends on both the reactivity and concentration of the intermediate Ru*. The resulting decisive role of both parameters work in opposite manners: Schiff base ligands with strong electron donating properties show a relatively weak arene coordination and Ru* is present in higher concentrations ($K_C > K_{NC}$). Though these systems produce intermediates with lower reactivities towards EDA, on the other hand, $k_{2,C} < k_{2,NC}$, because of the stabilizing effects of the ligand.

From the observed temperature dependence findings, we must conclude that the overall activity as a function of

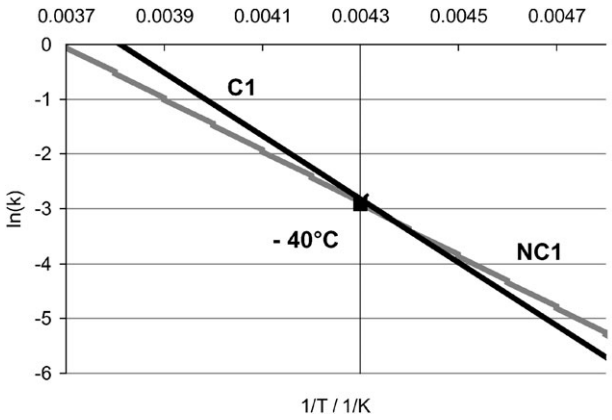

Fig. 5 Extrapolated Arrhenius plot of C1 and NC1.

temperature is determined by the reactivity of Ru* rather than by its concentration.

A practical implication of the difference in temperature dependence between catalysts **C1** and **NC1** is the predicted higher activity of the nitro systems at lower temperatures. From the crossover point of the Arrhenius plots (Fig. 5) we expect this crossover to occur below −40 °C. This explains why a lower activity in the decomposition of EDA was observed for catalyst **NC1** at operational temperatures, although a smaller value for $E_{a,calc}$ was also found. The temperature barely influenced the rate constant because of the high reactivity of the intermediary species when a NO_2-group was present. Compared with **C1**, it is logical that for a given temperature, there is a turnover in activity (Fig. 5).

TGA measurements revealed a strong *p*-cymene coordination for **C0** (Table 1), but looking at Fig. 4A, **C0** shows a remarkable activity compared to the Schiff base systems. In solution, the dimer easily tends to undergo cleavage of the **Cl** bridges. A reactive, threefold coordinated, 16 electron species with vacant sites is formed this way. Theoretically, no further decoordination of ligands is needed to start the reaction. Thus, in contrast with the Schiff base systems, the equilibrium is shifted in favour of the dissociated complex in the case of **C0** and thus $K_{C0} \ggg K_{SchiffBase}$. This explains the extraordinary decomposition activity of **C0**.

When the carbene transfer is performed under careful control of the reaction parameters (GC analysis), we have to conclude that the electronic properties of the Schiff base nitrogen atom (**C1–C4**) is not so clear, since all catalysts produce cyclopropane products in equally moderate yields and with a mediocre diastereoselectivity. Modifying the donating properties of the O atom by applying a NO_2-group in the *para* ring position resulted in a large observed decrease in both selectivity and diastereoselectivity. So taking into account the results for catalysts **C1** and **NC1**, as discussed above, we are able to extrapolate for other catalysts and concur that applying a *p*-NO_2 substituent to the salicyl ring produced more reactive intermediates, resulting in lower selectivities towards cyclopropanation. Nevertheless, comparing **C4** and **NC4**, the effect of the NO_2 group diminished when the donating properties of the imine nitrogen were relative weak. For the same reason the dimer **C0** showed lower selectivities.

The influence of the substrate on the decomposition of EDA was examined, but the differences were not noteworthy. This can be understood from the lack of selectivity when EDA was added all at once (Table 4, entry $\mathbf{C1}_{IR}$).

When EDA was added very slowly, the nature of the olefin had larger repercussions (Table 5). Electronically-activated olefins, such as styrenes, produced cyclopropanes in much higher selectivities than did non-activated olefins. The differences between the three styrene derivatives were typically small, although a decrease in selectivity when a chloro substituent was used is noteworthy. Diastereoselectivity was not influenced by the electronic effects of these substrates. Using *cis*-cyclooctene, very good diastereoselectivity results favoured the *trans* diastereomer. This was considered due to the α,β-substituted double bond and the rigidity of this substrate. Nevertheless, poor selectivity of cyclopropanation was observed when non-activated olefins were used. Metathesis reactions seem not to have occurred with these substrates under the conditions used.

4. Conclusions

Ru(II)–arene catalysts bearing Schiff base ligands are active catalysts in carbene chemistry and have proven their activity towards different reactions of metal carbenes. By controlling the reaction conditions, cyclopropanation could be favoured and side reactions, such as dimerisation and metathesis, suppressed.

We found that the electronic properties of the Schiff base ligand had a prevailing influence on the decomposition rate; the more donating the Schiff base, the faster the decomposition, but the less reactive the intermediates formed. This lower reactivity was responsible for the improved selectivities obtained when Schiff base ligands with strong electron donating properties were used. No indication of steric influence from the Schiff base ligands on reactions could be found, either for EDA decomposition or selective carbene transfer.

No strong conclusions could be drawn concerning the electronic or steric nature of the olefin for the catalytic decomposition of EDA. However, the electronic nature of the substrate did have strong repercussions on the selectivity of carbene transfer. Activated olefins resulted in a higher proportion of cyclopropanation products than did non-activated olefins.

5. Experimental

Synthesis

All materials were of analytical grade and used without further purification. The starting material (Ru-(*p*-cymene)Cl_2)$_2$ was synthesized according to the literature[7c,10b] (*p*-cymene = 4-isopropyltoluene). For the synthesis of the Schiff base ligands and catalysts we followed the work of the same researchers.[10a]

TGA measurements

TGA measurements were performed on a TA instrument, SDT 2960. The catalyst samples were placed under a He atmosphere and a heating rate of 10 °C min^{-1} applied. Thermodynamic parameters were obtained from the derivative of the TGA curve.

FT-IR measurements

Kinetic measurements were assessed by using a Bruker FT-Raman/FT-IR spectrometer with a Nernst glowing element as the IR source and a DTGS detector.

In a typical experiment, catalyst (1 μmol) and olefin (2.5 mmol) were dissolved in toluene (12.5 ml) in a 15 ml flask through a septum. At 0 °C, EDA (125 μmol) was added, the mixture heated up to the reaction temperature, and passed through an IR cell by the use of a peristaltic pump. Repeated measurements were performed by following the ν(N≡N) stretch at 2110 cm^{-1}. All spectra were background corrected, normalized to the solvent, integrated and correlated for concentration by means of a calibration curve. All experiments were repeated at least five times.

GC measurements

GC measurements were performed on a Varian CDS 401 with a Supelco 5DB-24030 capillary column and a FID detection system.

In a typical GC experiment, catalyst (5 μmol) was dissolved in olefin (12.5 mmol) in a 15 ml flask through a septum. EDA (625 μmol) dissolved in toluene (12.5 ml) was added over a period of 4 h using a peristaltic pump. After addition of a few drops of EDA solution, the mixture was heated from 0 °C to the reaction temperature. After complete addition, the mixture was kept at reaction temperature overnight. Analysis was performed by injecting an aliquot containing diethyl adipate as internal standard. The composition of the reaction mixture was fully characterized by MS, in comparison with authentic samples.

Acknowledgements

F. Verpoort is indebted to the FWO-Flanders (Fonds voor Wetenschappelijk Onderzoek-Vlaanderen) for financial support to the research funds of Ghent University.

References

1 (*a*) A. F. Noels, in *Applied Homogeneous Catalysis with Organometallic Compounds*, ed. B. Cornils and W. A. Herrmann, Wiley-VCH, New York, 2000, pp. 733–747; (*b*) M. P. Doyle, in *Comprehensive Organometallic Chemistry II*, ed. E. W. Abel, F. G. A. Stone, G. Wilkinson, Pergamon Press, Oxford, 1995, vol. **12**, pp. 387–420; (*c*) T. Aratani, Y. Yoneyoshi and T. Nagase, *Tetrahedron Lett*., 1975, **21**, 1707; (*d*) J. H. Simpson, J. Godfrey, R. Fox, A. Kotnis, D. Kacsur, J. Hamm, M. Totelben, V. Rosso, R. Mueller, E. Delaney and R. P. Deshpande, *Tetrahedron: Asymmetry*, 2003, **75**, 3569; (*e*) I. E. Marko, T. Giard, S. Sumida and A.-E. Gies, *Tetrahedron Lett*., 2002, **43**, 2317; (*f*) M. P. Doyle, *Chem. Rev*., 1986, **86**, 919; (*g*) D. Jan, F. Simal, A. Demonceau, A. F. Noels, K. A. Rufanov, N. A. Ustynyuk and D. G. Gourevitch, *Tetrahedron Lett*., 1999, **40**, 5695; (*h*) B. F. Straub, I. Gruber, F. Rominger and P. Hofmann, *J. Organomet. Chem*., 2003, **684**, 124.

2 (*a*) P. Yates, *J. Am. Chem. Soc*., 1952, **74**, 5376; (*b*) H. Nozaki, H. Takaya, D. Moriuti and R. Noyori, *Tetrahedron*, 1968, **24**, 3655; (*c*) B. W. Peace and S. Wulfman, *Tetrahedron Lett*., 1971, **41**, 3799; (*d*) R. G. Salomon and J. K. Kochi, *J. Am. Chem. Soc*., 1973, **95**, 3300; (*e*) A. J. Anciaux, A. J. Hubert, A. F. Noels, N. Petiniot and P. Teyssié, *J. Org. Chem*., 1980, **45**, 695; (*f*) A. F. Noels, A. Demonceau, E. Carlier, A. J. Hubert, R.-L. Máequez-Silva and R. A. Sánchez-Delgado, *J. Chem. Soc., Chem. Commun*., 1988, 783; (*g*) D. A. Evans, K. A. Woerpel, M. M. Hinman and M. M. Fauk, *J. Am. Chem. Soc*., 1991, **113**, 726; (*h*) M. P. Doyle, V. Bagheri, T. J. Wandless, N. K. Harn, D. A. Brinker, C. T. Eagle and K.-L. Loh, *J. Am. Chem. Soc*., 1990, **112**, 1906; (*i*) A. Demonceau, A. F. Noels, J.-L. Costa and A. J. Hubert, *J. Mol. Catal*., 1990, **58**, 21; (*j*) M. P. Doyle and I. M. Philips, *Tetrahedron Lett*., 2001, **42**, 3155.

3 (*a*) A. Demonceau, E. Saive, Y. de Froidmont, A. F. Noels and A. J. Hubert, *Tetrahedron Lett*., 1992, **33**, 2009; (*b*) G. Maas, T. Werle, M. Alt and D. Mayer, *Tetrahedron*, 1993, **49**, 881; (*c*) H. Nishiyama, Y. Itoh, H. Matsumoto, S.-B. Park and K. Itoh, *J. Am. Chem. Soc*., 1994, **116**, 2223; (*d*) A. Demonceau, F. Simal, A. F. Noels, C. Viñas, R. Nuñez and F. Teixidor, *Tetrahedron Lett*., 1997, **38**, 4079; (*e*) F. Simal, A. Demonceau, A. F. Noels, D. R. T. Knowles, S. O'Leary, P. M. Mitlis and O. Gusev, *J. Organomet. Chem*., 1998, **558**, 163; (*f*) F. Simal, A. Demonceau and A. F. Noels, *Tetrahedron Lett*., 1998, **39**, 3493; (*g*) C. Bianchini and H. M. Lee, *Organometallics*, 2000, **19**, 1833; (*h*) G. Maas and J. Seitz, *Tetrahedron Lett*., 2001, **42**, 6137; (*i*) G. Maas, *Chem. Soc. Rev*., 2004, **33**, 183.

4 (*a*) X. Yao, M. Qiu, W. Lu, H. Chen and Z. Zheng, *Tetrahedron: Asymmetry*, 2001, **12**, 197; (*b*) Z. Zheng, X. Yao, C. Li, H. Chen and X. Hu, *Tetrahedron Lett*., 2001, **42**, 2847; (*c*) J. A. Miller, W. Jin and S. T. Nguyen, *Angew. Chem., Int. Ed*., 2002, **41**, 2953; (*d*) O. Tutusaus, S. Delfosse, A. Demonceau, A. F. Noels, R. Nuñez, C. Viñas and F. Teixidor, *Tetrahedron Lett*., 2002, **43**, 983; (*e*) C. Bonaccorsi, S. Bachmann and A. Mezzetti, *Tetrahedron: Asymmetry*, 2003, **14**, 845; (*f*) H. Dai, X. Hu, H. Chen, C. Bai and Z. Zheng, *J. Mol. Catal. A: Chem*., 2004, **211**, 17; (*g*) A. Berkessel, P. Kaiser and J. Lex, *Chem.–Eur. J*., 2003, **9**, 4746; (*h*) C. Paul-Roth, F. De Montigny, G. Rethoré, G. Simonneaux, M. Gulea and S. Masson, *J. Mol. Catal. A: Chem*., 2003, **201**, 79; (*i*) E. Galardon, P. Le Maux and G. Simmonneaux, *Chem. Commun*., 1997, **10**, 927; (*j*) M. Frauenkron and A. Berkessel, *Tetrahedron Lett*., 1997, **41**, 7175.

5 (*a*) H.-L. Wong, S.-J. Jeon, H.-S. Kim, C.-S. Cho, S.-C. Shim and T.-J. Kim, *Tetrahedron: Asymmetry*, 1999, **10**, 3833; (*b*) H. L. Wong, Y. Tian and K. S. Chan, *Tetrahedron Lett*., 2000, **41**, 7723; (*c*) M. Schinnerl, C. Böhm, M. Seitz and O. Reiser, *Tetrahedron: Asymmetry*, 2003, **14**, 765; (*d*) P.-F. Teng, T.-S. Lai, H.-L. Kwong and C. M. Che, *Tetrahedron: Asymmetry*, 2003, **14**, 837; (*e*) M. P. Doyle and J. Colyer, *J. Mol. Catal. A: Chem*., 2003, **196**, 93; (*f*) P. Tagliatesta and A. Pastorini, *J. Mol. Catal. A: Chem*., 2003, **198**, 57.

6 (*a*) J.-L. Zhang, P. W. H. Chan and C. M. Che, *Tetrahedron Lett*., 2003, **44**, 8733; (*b*) L. He, P. W. H. Chan, W. M. Tsui, W. Y. Yu and C. M. Che, *Org. Lett*., 2004, **6**, 2405; (*c*) Z. Y. Zhou, W. Y. Yu, P. W. H. Chan and C. M. Che, *J. Org. Chem*., 2004, **69**, 7072; (*d*) G. Y. Li and C. M. Che, *Org. Lett*., 2004, **6**, 1621.

7 (*a*) B. De Clercq and F. Verpoort, *Catal. Lett*., 2002, **83**, 9; (*b*) B. De Clercq and F. Verpoort, *J. Mol.Catal. A: Chem*., 2002, **180**, 67; (*c*) B. De Clercq, PhD Thesis, Ghent University, Belgium, 2003.

8 A. F. Noels, A. Demonceau and D. Jan, *Russ. Chem. Bull*., 1999, **48**, 1206.

9 R. D. Hancock and A. E. Martell, *Chem. Rev*., 1989, **89**, 1875.

10 (*a*) T. Opstal, K. Melis and F. Verpoort, *Catal. Lett*., 2001, **74**, 155; (*b*) T. Opstal, PhD Thesis, Ghent University, Belgium, 2003.

11 W. Baratta, W. A. Herrman, R. M. Kratzer and P. Rigo, *Organometallics*, 2000, **19**, 3664.

12 (*a*) M. C. Pirrung and A. T. Morehead, *J. Am. Chem. Soc*., 1996, **118**, 8162; (*b*) M. C. Pirrung, H. Liu and A. T. Morehead, *J. Am. Chem. Soc*., 2002, **124**, 1014.